Table S1 : Depth of the base of Pliocene in boreholes or outcrops. Depth values are in meter.

Borehole name	Longitude (DD.ddd)	Latitude (DD.ddd)	BSS_ID	Borehole ground level (m)	Borehole depth (m)	Quaternary thickness (m)	Depth of Pliocene base in borehole (m)	Pliocene thickness (m)	MES hypsometry (m)	Pliocene base	Underlying formation
Mangarele	4.587058	44.254152	BSS002CLER	105.0	34.3	3.0			105.0	No Pliocene	Cenomanian
Mirabelle	4.695492	44.302295	BSS002BNPG	46.0	21.0	13.4			46.0	No Pliocene	Cenomanian
Chemin de Grignan	4.746070	44.324388	BSS002BNQM	61.0	75.0	6.0			5.0	No Pliocene	Cenomanian
Suze-la-Rousse	4.843029	44.292469	BSS002BPLF	82.0	1342.0	6.8			75.2	No Pliocene	Burdigalian
Ste-Cecile-Les-Vignes	4.877293	44.253148	BSS002CMGN	108.0	86.0				108.0	No Pliocene	Miocene
La Prade	4.597795	44.259322	BSS002CLED	88.0	110.3	17.0			71.0	No Pliocene	Turonian
Preference	4.708228	44.279152	BSS002CLTY	45.0	30.0	10.0			46.0	No Pliocene	Turonian
Grand Malijac	4.668954	44.302953	BSS002BMYX	44.0	70.0	3.0			44.0	No Pliocene	Turonian
Donzere channel	4.744058	44.304655	BSS002BNNV	59.5	60.0	15.0			51.0	No Pliocene	Turonian
Pierrelatte rock	4.697774	44.377961	Outcrop	56.0	11.0				56.0	No Pliocene	Urgonian
Donzere Dam	4.678171	44.439168	BSS002BNDW	65.0	9.5				65.0	No Pliocene	Urgonian
Donzere Dam	4.679224	44.439476	BSS002BNDF	57.3	9.6				57.3	No Pliocene	Urgonian
Donzere Dam	4.679106	44.439965	BSS002BNDG	57.3	10.2				57.3	No Pliocene	Urgonian
Donzere Dam	4.679972	44.440169	BSS002BNDL	56.9	13.2				56.9	No Pliocene	Urgonian
Donzere Dam	4.681230	44.440242	BSS002BNDH	56.7	10.1				56.7	No Pliocene	Urgonian
Donzere Dam	4.682528	44.440618	BSS002BNDJ	56.7	19.0				56.7	No Pliocene	Urgonian
Donzere Dam	4.684804	44.441375	BSS002BNDK	57.5	14.3				57.5	No Pliocene	Urgonian
Donzere Dam	4.694056	44.442093	BSS002BNDD	58.2	16.3	15.0			43.2	No Pliocene	Urgonian
Donzere Dam	4.697399	44.444410	BSS002BNDE	57.4	29.3	26.0			31.4	No Pliocene	Urgonian
Gerige	4.634292	44.371313	BSS002BMSE	143.5	92.0				143.5	No Pliocene	Aptian
Donzere Dam	4.744460	44.313459	BSS002BNPC	55.1	18.0	13.0			56.0	No Pliocene	Cenomanian
Gignoux	4.762750	44.285626	BSS002BNPF	62.0	190.0	12.0	190.0	178.0	Below -128 m	Pliocene base below bottom	Unknown
Coulorgues	4.684661	44.205054	BSS002CLYU	36.0	80.0	12.8	63.0	50.2	Below -24 m	Pliocene base below bottom	Unknown
Les Tuilleres	4.654339	44.247283	BSS002CLGL	40.0	277.0	12.0	303.0	291.0	Below -263 m	Pliocene base below bottom	Unknown
Bollene-J-Vernes	4.756039	44.287210	BSS002BNPJ	60.0	190.0	12.0	190.0	178.0	Below -130 m	Pliocene base below bottom	Unknown

Combe-Briard	4.641569	44.367259	BSS002BMYM	72.0	40.0	13.0	40.0	27.0	Below 32 m	Pliocene base below bottom	Unknown
Donzere Dam	4.740171	44.422791	BSS002BNBL	81.8	100.0	5.0	100.0	95.0	Below -18.2 m	Pliocene base below bottom	Unknown
Donzere Dam	4.679114	44.436760	BSS002BNDN	57.1	30.0	17.0	30.0	13.0	Below 27 m	Pliocene base below bottom	Unknown
Donzere Dam	4.682687	44.437498	BSS002BNDM	57.7	34.0	10.0	34.0	24.0	Below 23.65 m	Pliocene base below bottom	Unknown
Codolet	4.700617	44.129745	BSS002CMTA	32.0	451.0	7.2	451.0	443.8	Below-419 m	Pliocene base below bottom	Unknown
Parot	4.609903	44.323370	BSS002BMYK	125.0	78.0	15.0	78.0	63.0	Below 47 m	Pliocene base below bottom	Unknown
Sica	4.642544	44.247242	BSS002CLEG	57.0	117.0	15.0	80.0	65.0	Below - 23 m	Pliocene base below bottom	Bottom in MTD facies
Pont de Bourg	4.648702	44.368532	BSS002BMXR	57.0	42.0	8.7	42.0	33.3	Below 15 m	Pliocene base below bottom	Unknown
St-Paul-Trois-Chateaux	4.736043	44.346733	BSS002BNWH	58.0	834.0	6.0	462.0	456.0	-406.0	Pliocene base within borehole	Aptian
Pierrelatte	4.725810	44.379203	BSS002BNBB	56.0	351.0	22.0	291.0	269.0	-234.0	Pliocene base within borehole	Aptian
Mondragon	4.731982	44.248986	BSS002CLTG	50.3	1838.0	12.0	93.0	81.0	-43.0	Pliocene base within borehole	Cenomanian
La Siolle	4.592058	44.270974	BSS002CLEE	68.0	94.0	19.5	85.0	65.5	-19.0	Pliocene base within borehole	Cenomanian
La Siolle	4.594226	44.271964	BSS002CLCA	64.0	151.0	6.0	104.0	98.0	-43.0	Pliocene base within borehole	Cenomanian
Sica	4.591855	44.272673	BSS002CLEL	63.0	152.8	12.0	129.0	117.0	-65.0	Pliocene base within borehole	Cenomanian
La Grangette	4.604262	44.273661	BSS002CLEB	50.0	290.5	8.0	150.0	142.0	-90.0	Pliocene base within borehole	Cenomanian
Les Mattes Nègres	4.891007	44.267625	BSS002CMCX	125.0	2.8	6.0	87.0	81.0	38.0	Pliocene base within borehole	Miocene
Les Fourches	4.803335	44.274709	BSS002PZXX	82.0	200.0	4.0	133.0	129.0	-47.0	Pliocene base within borehole	Miocene or U. Cretaceaous
Canuels	4.598406	44.262192	BSS002CLEC	81.0	133.2		34.0	34.0	47.0	Pliocene base within borehole	Table for Paper
Breteau	4.582673	44.263687	BSS002CLBB	80.0	167.6		31.0	31.0	52.0	Pliocene base within borehole	Turonian
Suze-la-Rousse	4.598722	44.265767	BSS002CLEA	64.0	159.5		60.0	60.0	3.0	Pliocene base within borehole	Turonian
La Begude	4.600223	44.267108	BSS002CLFA	64.0	102.0		41.0	41.0	23.0	Pliocene base within borehole	Turonian
Sica	4.590988	44.273383	BSS002CLEJ	67.0	193.0	9.0	72.0	63.0	-6.0	Pliocene base within borehole	Turonian
Coste-Belle	4.790413	44.288152	BSS002BPMF	74.0	56.0	4.0	39.0	35.0	34.0	Pliocene base within borehole	Turonian
Ilette	4.640573	44.308735	BSS003XIZU	46.0	278.0	18.0	200.0	182.0	-154.0	Pliocene base within borehole	Cenomanian

Figure S1: Location of seismic lines studied on a simplified geological map, in addition to boreholes used for analysis and construction of the MES model (see Table S1).

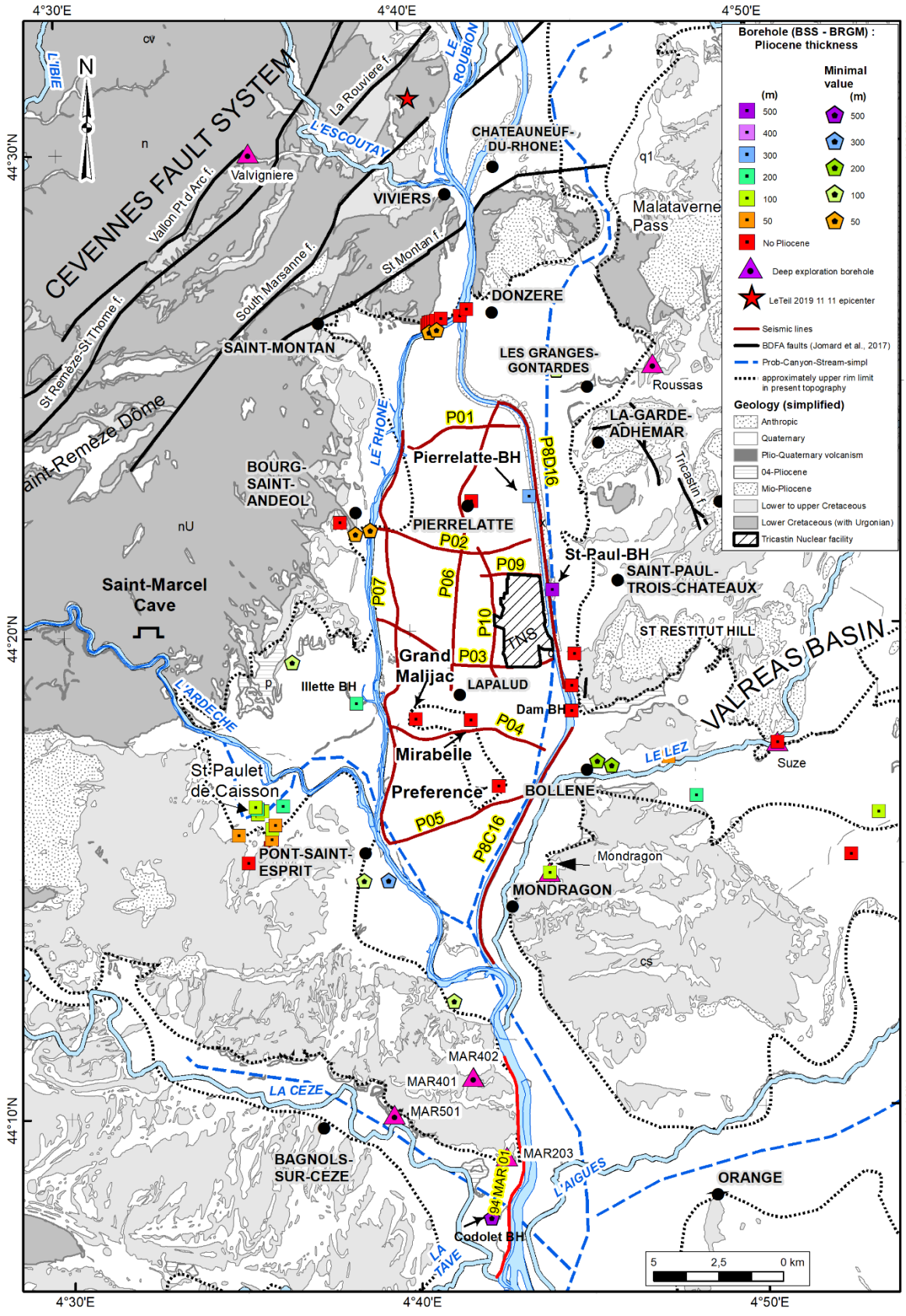

Methodology of depth correction using deep statics

The depth conversion of seismic units necessitates the utilization of velocity data. To this end, seismic reprocessing was undertaken on seismic line P4, strategically chosen for its intersection with two canyons and an intermediate island formed by Cretaceous-age series, as evidenced by three boreholes (Grand-Malijac, Mirabelle, and Préférence; see Fig. 4, 5).

The distinctive geology characterized by deep erosion poses a challenge to seismic imaging in the time domain due to the marked contrast in velocities between the canyon filling units (exhibiting low velocities) and the surrounding formations (typically characterized by high velocity units). This velocity contrast persists over considerable thicknesses, complicating seismic imaging and giving rise to various issues that cannot be remedied by conventional depth processing (PreStack Depth migration) alone. These “temporal” issues include pull-down effects or cycle skips on the units, potentially leading to misinterpretations such as misidentification of faults (due to cycle skips) or false structural assessments (anticline structural shape instead of monoclinal shape).

To address these challenges in seismic imaging, an innovative methodology developed by CDP Consulting was employed, focusing on delineating the shape of the Ardèche and Rhône paleo-valleys, determining the P-wave velocities of the Messinian canyon filling units and the surrounding formations. This involved a two-step processing approach.

Firstly, a conventional time seismic processing was conducted to reconstruct the Pliocene filling horizons, a task previously undertaken by the CDP company for EDF, optimized through data exchange and further enhancements (Figure S2).

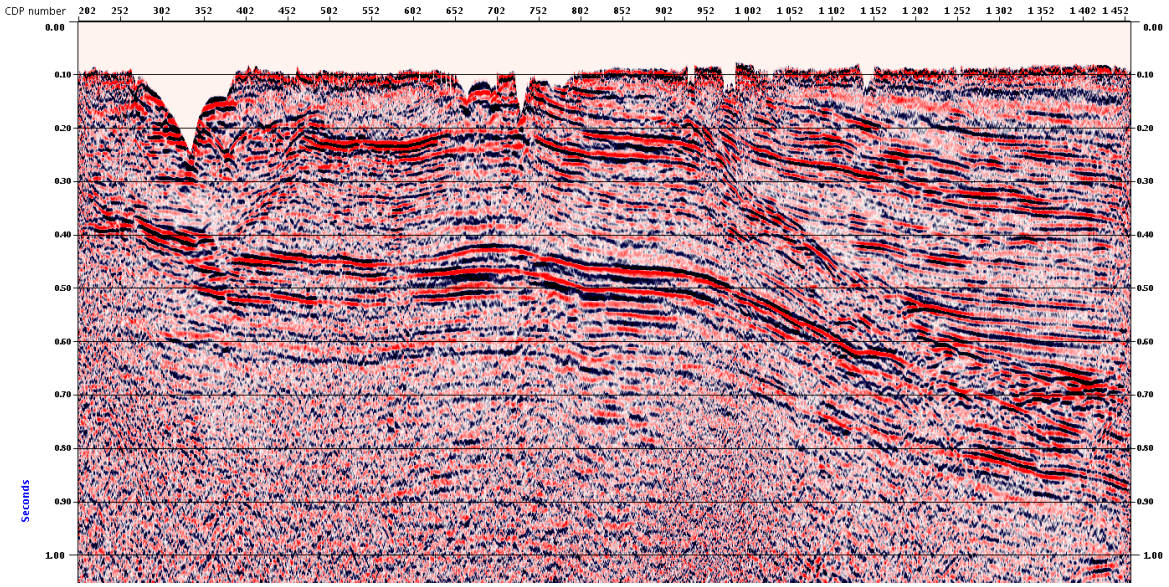

Figure S2: Stack in time after conventional processing.

Secondly, a "deep" processing developed by CDP Consulting, incorporating "deep statics," was implemented to rectify temporal effects caused by the canyon on underlying units, thereby restoring the true structural shape at depth across all horizons along the seismic profile. The deep statics computation involved introducing a time correction before stacking to mitigate the adverse effects of velocity contrast between the canyon filling units and the faster velocity Cretaceous units. To master the computation of these “deep” statics, velocity parameters and layer geometry are crucial information.
Constant velocity stacks were initially created to model P-wave interval velocities of different

geological formations, facilitating differentiation of units with similar seismic facies. Based on this differentiation and the analysis of constant velocity stacks, a scalable interval velocity model was generated (Figure S3), yielding several iterative time/interval velocity models. These models were then converted into a stack velocity formula (RMS velocity) utilizing a derivative of the Dix formula (Figure S4). Subsequent testing of these RMS velocities in the stack process validated the input interval velocity model.

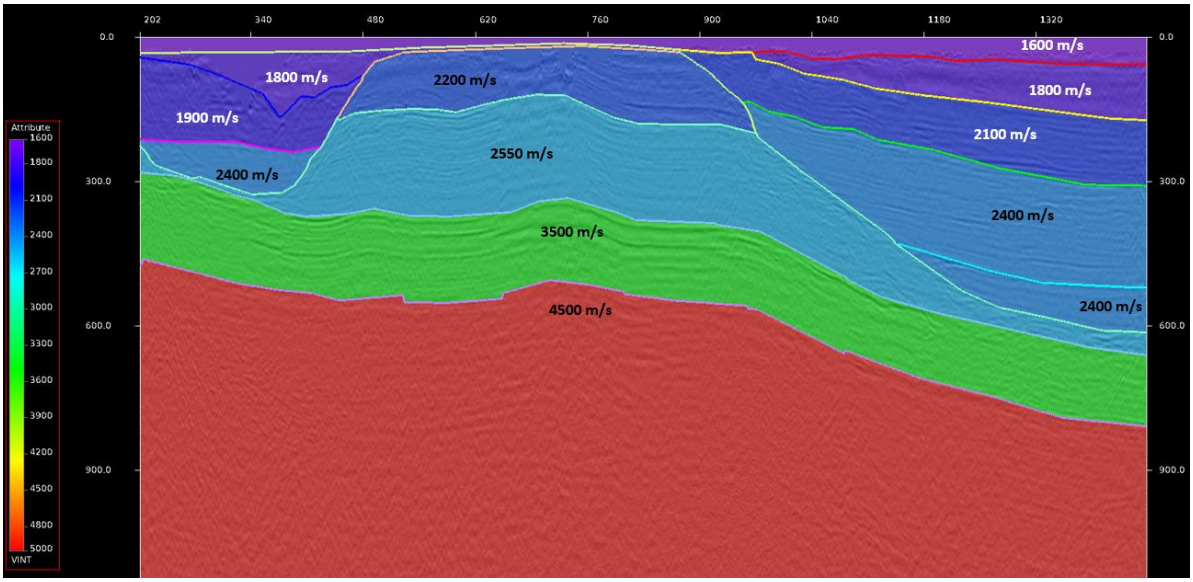

Figure S3: Final interval velocity model.

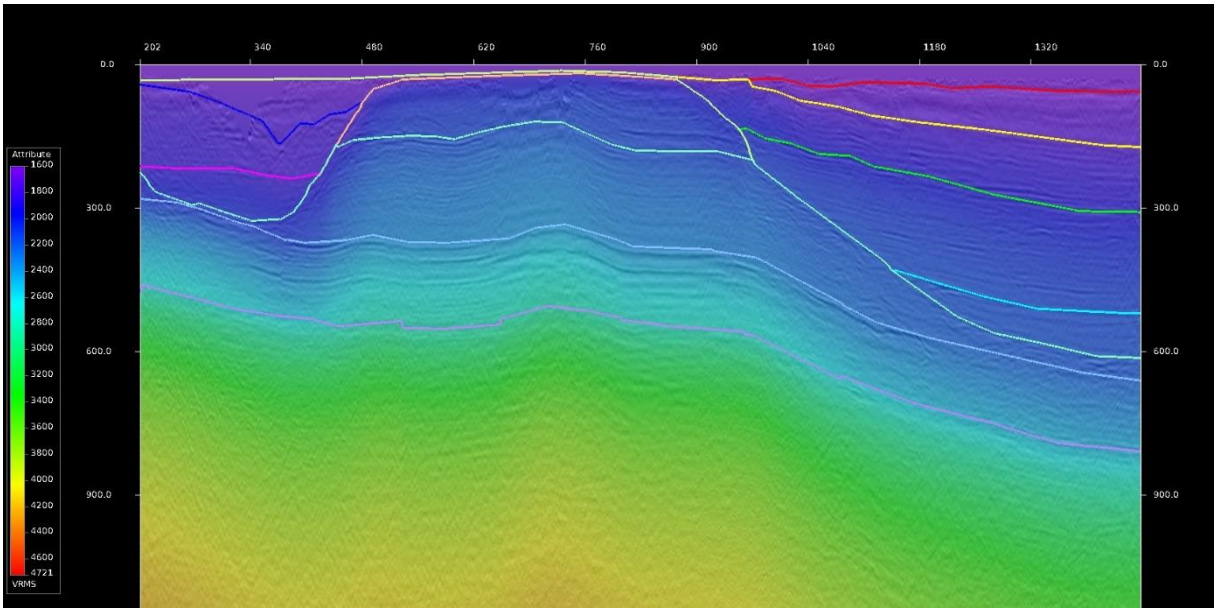

Figure S4: RMS velocity model derivated from the time based interval velocity model that has been tested in a stack process to validate its reliability.

Once the geometry of canyons and interval velocities of all seismic units were established, "deep processing" commenced. Deep statics, introduced in the processing as a prestack process on shots and receivers, aimed to correct lateral velocity contrasts observed within the "vertical" range of Messinian erosion. These deep statics were modeled based on results from the interval velocity modeling conducted earlier. Furthermore, the interval velocity model facilitated the description of canyon filling unit velocities and enabled the definition of a replacement velocity based on the mean velocity computed at the base of a reflector in time preserved from Messinian erosion (Urgonian).

A subsequent stack, incorporating these deep statics, resulted in a marked improvement in stack quality, particularly evident at the base of the Paleo-Ardèche (Figure S5), where conventional processing proved inadequate. Moreover, it restored structural imagery in time, aligning with real structural imagery in depth, revealing a nearly uniform dip of formations from west to east for Upper Cretaceous formations. It's worth noting that these Cretaceous formations, mimicking an anticlinal shape in the initial processing (without deep statics), were influenced by "pull-down" effects attributed to the low velocities of filling units of the Paleo-Rhône and Paleo-Ardèche.

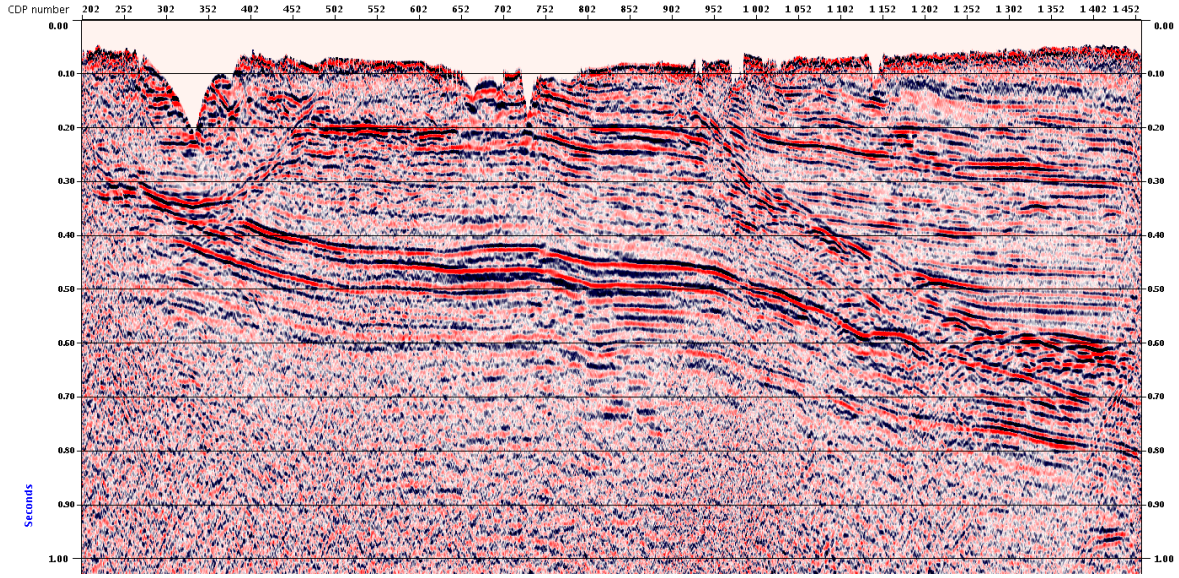

Figure S5: Stack with « deep » statics in time => improvement of the quality of the stack under the Paleo-Ardèche canyon

Finally, the resultant time stack, enhanced through the incorporation of "deep" statics, underwent conversion back to depth utilizing the generated interval velocity model.

Figure S6: Comparison of the MES surface at depth from Roure et al. (2009) and our new model of the MES at depth. We used the same color-scales for both maps. Note the different course of the ardèche and Rhône rivers.

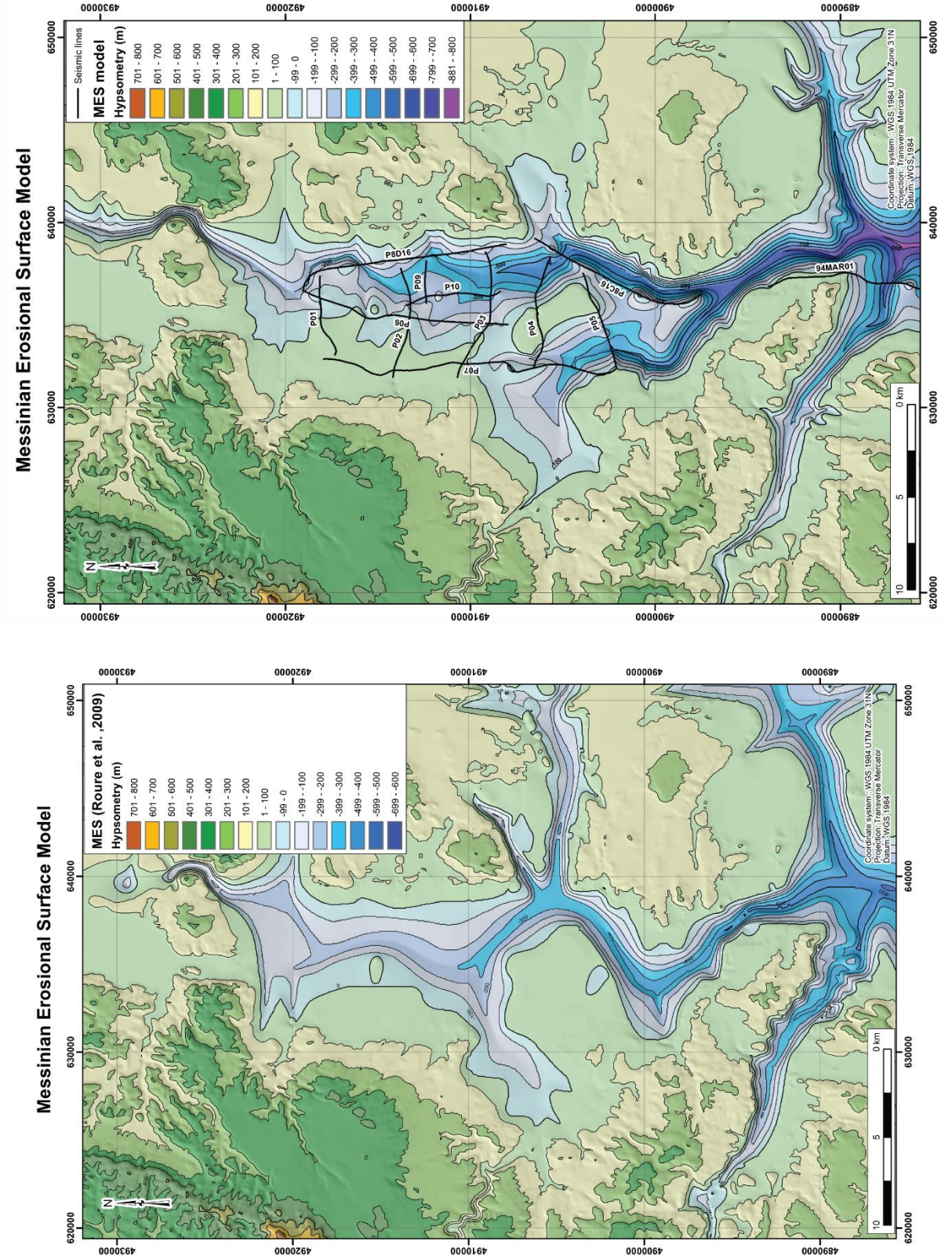

Figure S7: Uninterpreted seismic lines used in this manuscript.

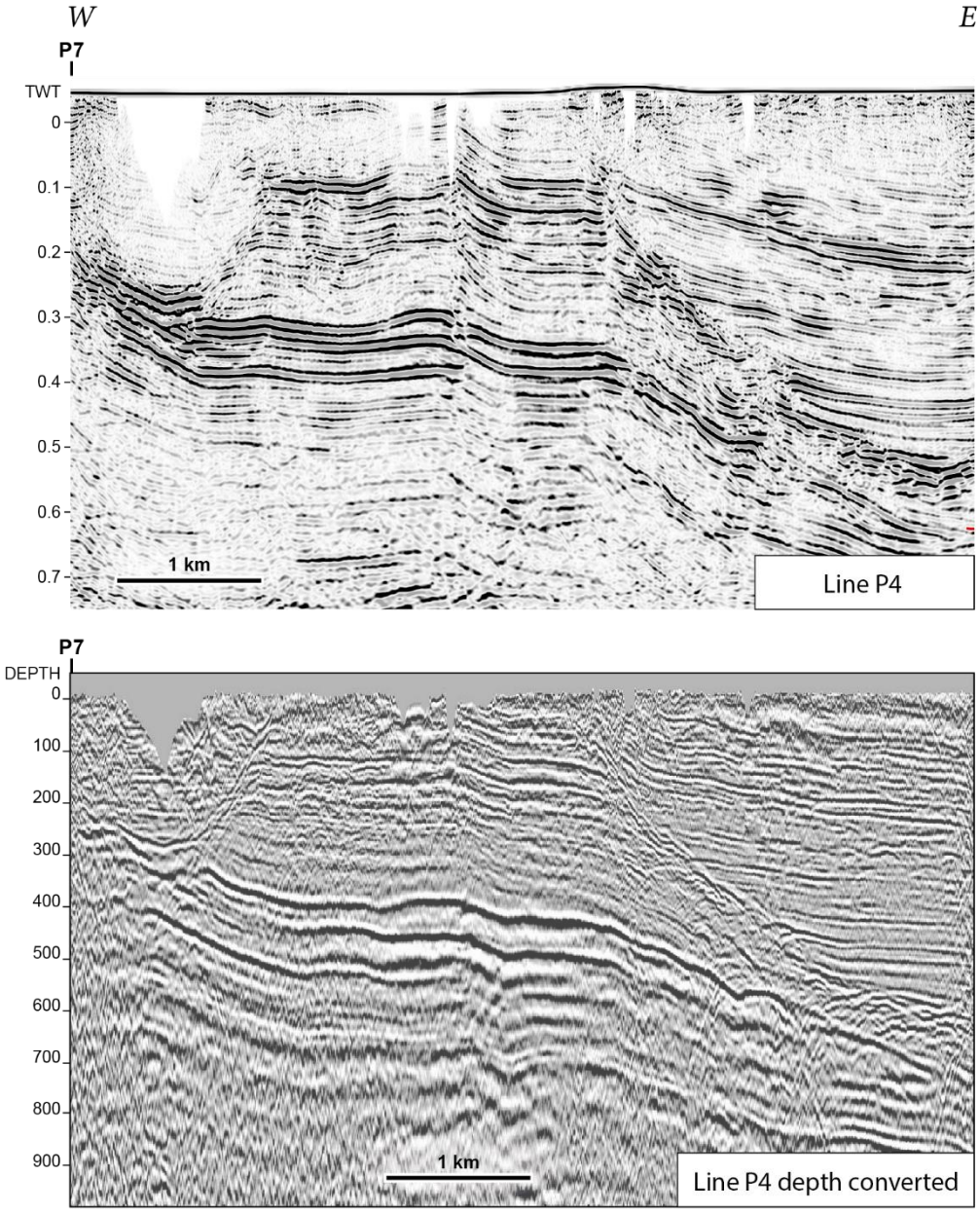

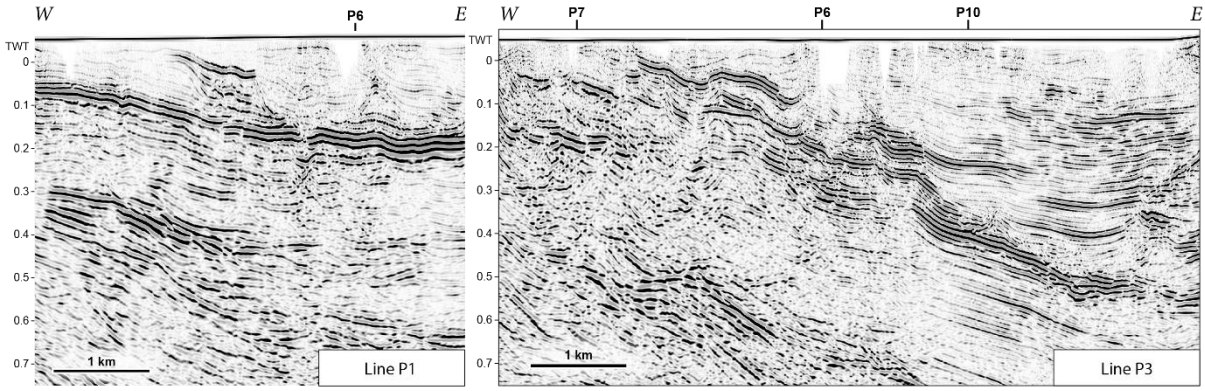
W
P6
E
TWT
0
0.1
0.2
0.3
0.4
0.5
0.6
0.7
1 km
Line P1

W
P7
P6
P10
E
TWT
0
0.1
0.2
0.3
0.4
0.5
0.6
0.7
1 km
Line P3

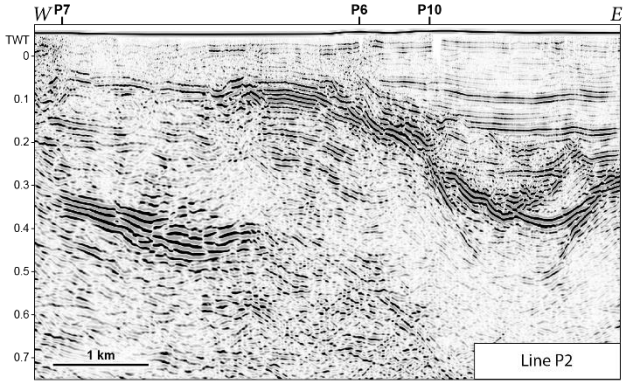
W
P7
P6
P10
E
TWT
0
0.1
0.2
0.3
0.4
0.5
0.6
0.7
1 km
Line P2

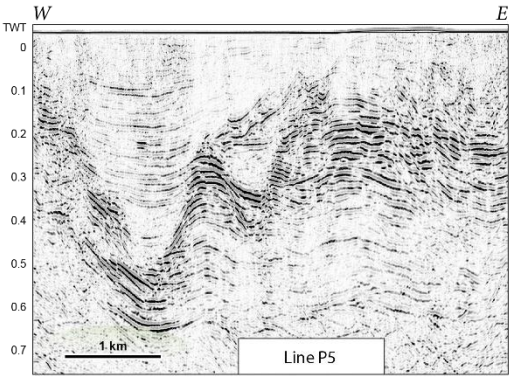
W
E
TWT
0
0.1
0.2
0.3
0.4
0.5
0.6
0.7
1 km
Line P5

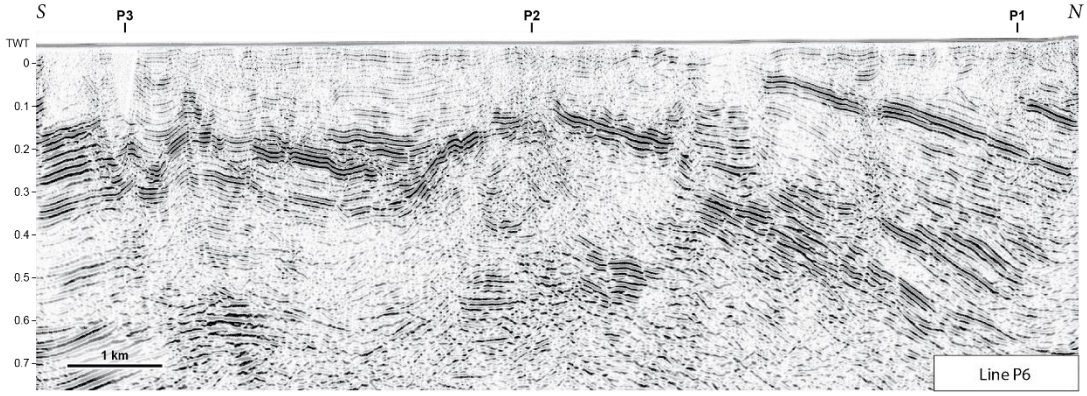
S
P3
P2
P1
N
TWT
0
0.1
0.2
0.3
0.4
0.5
0.6
0.7
1 km
Line P6

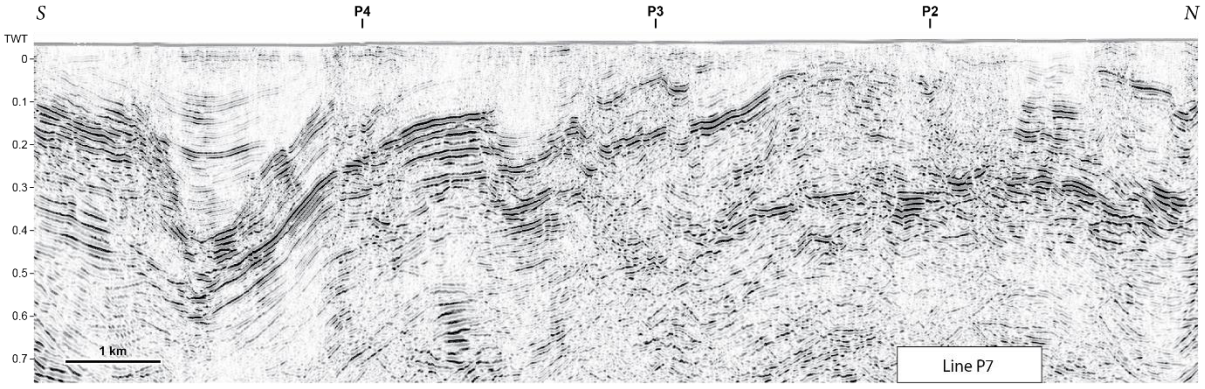
S
P4
P3
P2
N
TWT
0
0.1
0.2
0.3
0.4
0.5
0.6
0.7
1 km
Line P7

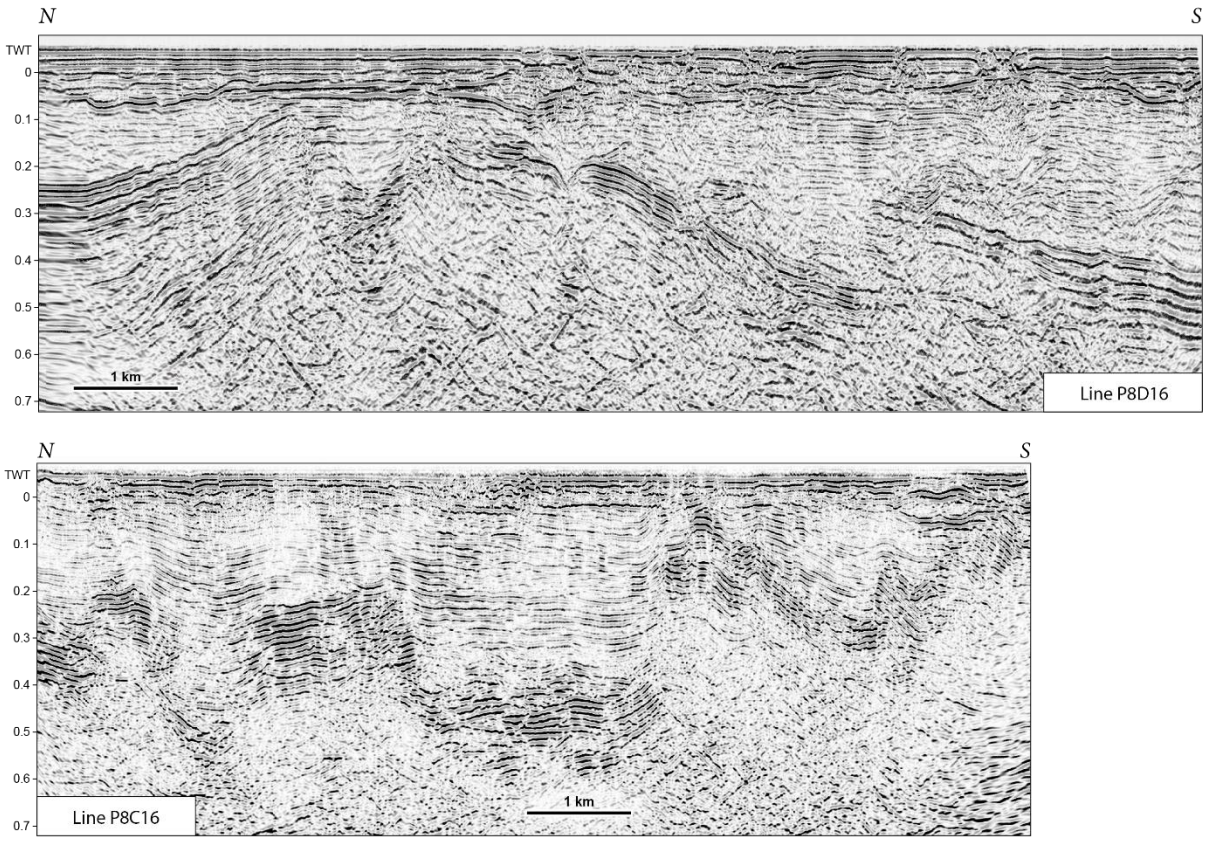
N
S
TWT
0
0.1
0.2
0.3
0.4
0.5
0.6
0.7
1 km
Line P8D16
N
S
TWT
0
0.1
0.2
0.3
0.4
0.5
0.6
0.7
Line P8C16
1 km

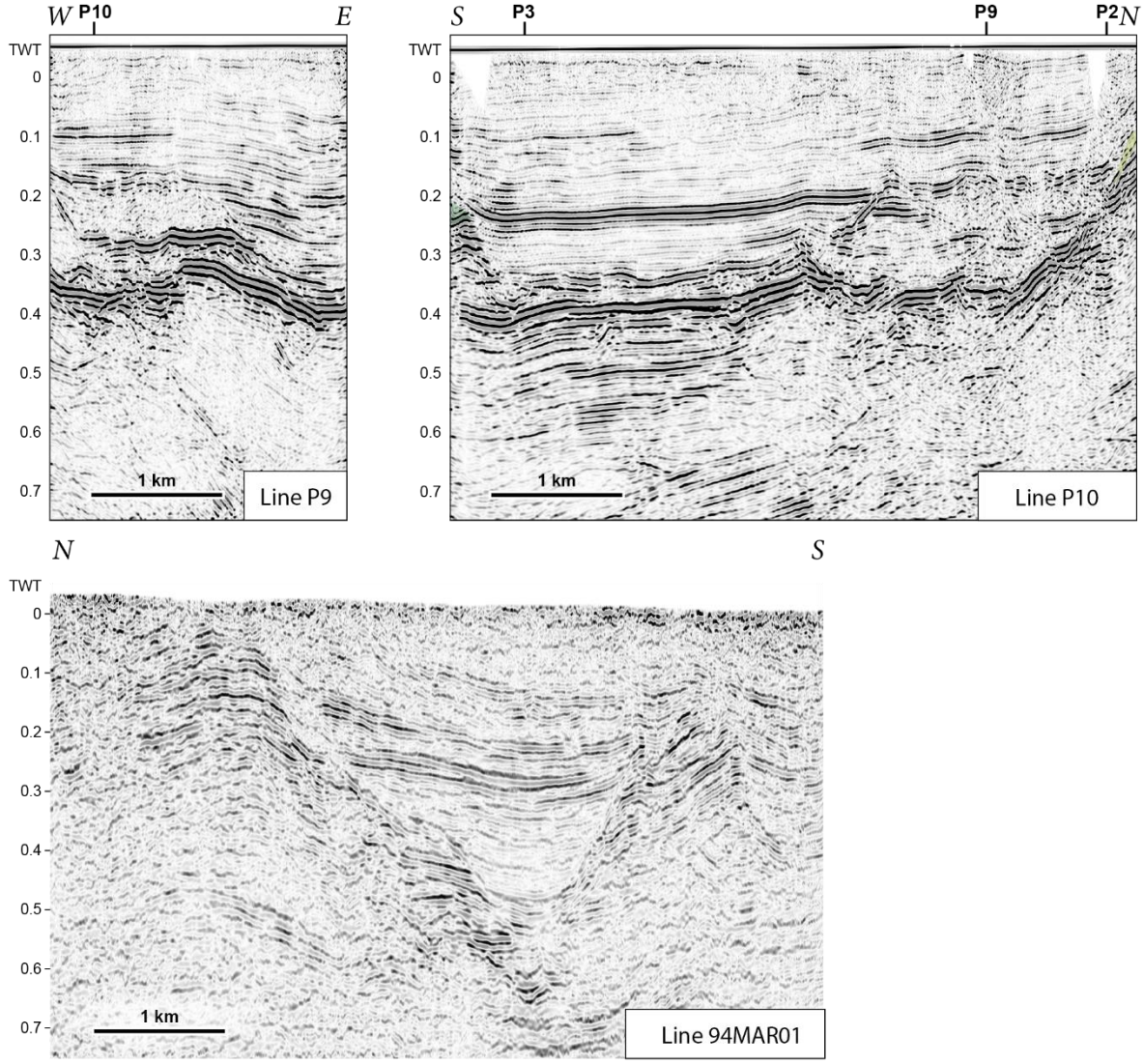
W
P10
E
TWT
0
0.1
0.2
0.3
0.4
0.5
0.6
0.7
1 km
Line P9
S
P3
P9
P2
N
TWT
0
0.1
0.2
0.3
0.4
0.5
0.6
0.7
1 km
Line P10
N
S
TWT
0
0.1
0.2
0.3
0.4
0.5
0.6
0.7
1 km
Line 94MAR01